ELSEVIER

30 June 1995

Chemical Physics Letters 240 (1995) 304–314

CHEMICAL PHYSICS LETTERS

High-order echoes in vibrational spectroscopy of liquids

Vadim Khidekel, Shaul Mukamel

Department of Chemistry, University of Rochester, Rochester, NY 14627, USA

Received 27 February 1995; in final form 8 May 1995

Abstract

Multidimensional infrared and Raman spectroscopy of liquids conducted using sequences of femtosecond pulses may be used to directly probe intramolecular and intermolecular nuclear motions. These techniques provide an additional insight into the nature of the nuclear spectral density observed in optical Kerr measurements. Photon echoes predicted in these systems are calculated and analyzed using multilevel coherences.

1. Introduction

Vibrational spectroscopy is a powerful tool for studying the molecular and atomic structure of condensed phases. Considerable efforts have been made to interpret infrared and Raman experiments and extract valuable information from vibrational line shapes [1–4]. Line broadening induced by dephasing processes is usually classified as either homogeneous or inhomogeneous [2,3]. Homogeneous broadening is due to the interaction between molecules or atoms and a bath with a very fast time scale. Inhomogeneous broadening, on the contrary, comes from the variation in transition frequencies for different molecules, as a result of different static local environments or initial states. Hence, inhomogeneous broadening carries no dynamic information. It is sometimes easy to separate these two mechanisms, but usually this is a complicated problem.

Linear optical experiments cannot distinguish between homogeneous and inhomogeneous broadening, since the signal is determined by their convolution [5]. However, nonlinear techniques such as fluorescence line narrowing [6], hole burning [1,7,8], or photon echoes [9–12] can detect these contributions separately. The photon echo technique enables us to eliminate the inhomogeneous contribution to line broadening and elicit the dynamic information hidden underneath the broad envelope obtained in linear absorption. Photon echo is an ideal time-domain technique that can be successfully carried out with very short pulses. One advantage it has over fluorescence line narrowing and hole burning resides in the fact that the signal is generated by all the molecules of a sample and not only by a small portion selectively excited by a narrow-band pulse. As a result, the sensitivity of the method is enhanced. The essence of the photon echo technique lies in the competition of dephasing and rephasing processes and controlling the phases gained in each evolution period. When the time delays between the pulses satisfy certain relations, these phases are equal, and inhomogeneous broadening is totally eliminated.

All of these arguments apply to the basic model of nonlinear optics in which the system is described as two vibrational levels coupled to a bath [13]. Vibrational spectroscopy of molecular liquids cannot be described

SSDI 0009-2614(95)00546-3

by this model. A more reasonable starting point is to consider nuclear motions in liquids using a continuous distribution of oscillators with a given spectral density [11,12]. The oscillator model is more complicated since multilevel dynamics and coherences may show up. An additional complication is that in condensed phases nuclear motion is characterized by a broad range of time scales, i.e. the spectral density is a continuous distribution of oscillators. Due to the lack of a clear separation of nuclear motions into 'fast' and 'slow', the notions of homogeneous and inhomogeneous broadening, as used traditionally in nonlinear optics, do not apply. It is not clear whether photon echoes are to be expected and what is their information content. A new way of thinking about these effects in terms of oscillators and spectral densities is necessary. Such a model was proposed in Ref. [5], where it was shown how photon echoes can be observed. In this Letter we study this problem further. We first present a simple derivation based on the coherent state (rather than the path integral) representation. Second we analyze the resulting echoes in terms of the sum over states expression and identify the relevant double-sided Feynman diagrams. The same formalism can be applied to infrared and off-resonant Raman measurements. The only difference is that in the former case we need consider correlation functions of the dipole operator, whereas in the latter we use the electronic polarizability. We will therefore use the infrared terminology, but all the results can be applied to the Raman case as well.

In Section 2 we introduce formal expressions for nonlinear response functions in Liouville space. In Section 3 we calculate these response functions for a model of single nuclear mode with an exponential dependence of the dipole operator on the nuclear coordinate. In Section 4 we add inhomogeneous broadening by using a Brownian oscillator model with a static distribution of parameters and show that a number of echo signals may be seen for the second- and third-order nonlinear response.

2. Nonlinear response functions in Liouville space

We consider a molecular liquid interacting with an external electric field. The Hamiltonian is

$$H = H_0 - E(\boldsymbol{r},t)V, \tag{1}$$

where H_0 is the electronic and nuclear molecular Hamiltonian and the dipole operator V represents its interaction with the field.

Optical signals are related to the polarization of the medium induced by the external radiation field,

$$P(\boldsymbol{r},t) = \mathrm{Tr}\,[V\rho(t)] \equiv \langle\langle V|\rho(t)\rangle\rangle, \tag{2}$$

where $|\rho(t)\rangle\rangle = \sum_{jk}\rho_{ik}(t)|jk\rangle\rangle$ and the ket $|jk\rangle\rangle$ denotes the Liouville-space operator $|j\rangle\langle k|$.

We next expand $\rho(t)$ in powers of electric field and define $P^{(n)}(\boldsymbol{r},t)$ as contribution to $P(\boldsymbol{r},t)$ to nth power in the field. We thus obtain

$$P(\boldsymbol{r},t) = \int_0^\infty \mathrm{d}t_n \int_0^\infty \mathrm{d}t_{n-1}\ldots\int_0^\infty \mathrm{d}t_1\, S^{(n)}(t_n,t_{n-1},\ldots,t_1)E(\boldsymbol{r},t-t_n)\ldots E(\boldsymbol{r},t-t_n-\ldots-t_1), \tag{3}$$

where

$$S^{(n)}(t_n,t_{n-1},\ldots,t_1) \equiv \left(\frac{\mathrm{i}}{\hbar}\right)^n \langle\langle V|\mathcal{G}(t_n)\mathcal{V}\mathcal{G}(t_{n-1})\mathcal{V}\ldots\mathcal{G}(t_1)\mathcal{V}\rho(-\infty)\rangle\rangle. \tag{4}$$

The Liouville-space operator $\mathcal{V}$ acts on an ordinary operator A through the commutator

$$\mathcal{V}A = [V,A],$$

and $\mathcal{G}(\tau)$ is the Liouville-space Green function for the system without the radiation field,

$$\mathcal{G}(\tau) = \theta(\tau) \exp\left(-\frac{\mathrm{i}}{\hbar}\mathcal{L}\tau \right), \qquad \mathcal{L} \equiv [H, A].$$

In this notation the three lowest-order response functions are

$$S^{(1)}(t_1) = \frac{\mathrm{i}}{\hbar}\langle\langle V|\mathcal{G}(t_1)\mathcal{V}\rho(-\infty)\rangle\rangle,$$

$$S^{(2)}(t_2, t_1) = \left(\frac{\mathrm{i}}{\hbar}\right)^2 \langle\langle V|\mathcal{G}(t_2)\mathcal{V}\mathcal{G}(t_1)\mathcal{V}\rho(-\infty)\rangle\rangle,$$

$$S^{(3)}(t_3, t_2, t_1) = \left(\frac{\mathrm{i}}{\hbar}\right)^3 \langle\langle V|\mathcal{G}(t_3)\mathcal{V}\mathcal{G}(t_2)\mathcal{V}\mathcal{G}(t_1)\mathcal{V}\rho(-\infty)\rangle\rangle. \tag{5}$$

The function $S^{(1)}(t_1)$ controls all linear optical measurements. In the remainder of this Letter we focus on the first two nonlinear response functions, $S^{(2)}(t_2, t_1)$ and $S^{(3)}(t_3, t_2, t_1)$.

Knowing $S^{(n)}(t_n, \ldots, t_1)$, we have all the information to predict n-wave mixing measurements. To obtain an explicit expressions for $S^{(n)}$ we need to introduce a specific model of the material system. This will be done next.

3. Response function of a single harmonic nuclear mode

We now apply the general formulas (5) to the case in which nuclear motions are represented by a single harmonic degree of freedom. We use the Hamiltonian in the form

$$H_0 = \hbar\omega_0\left(a^\dagger a + \tfrac{1}{2}\right), \tag{6}$$

where $a^\dagger$ and a are the creation and annihilation operators, respectively. We also need to specify how the dipole operator V depends on nuclear coordinates. In the case $V(q) = \alpha q$ the response is linear, and all $S^{(n)}(t_n, \ldots, t_1)$ vanish for $n > 1$. A simple nonlinear form that we will use in the present work is the exponential dependence,

$$V(q) = V_0 \mathrm{e}^{\alpha q}.$$

This model is very useful, since it enables us to describe also arbitrary polynomial dependencies of V on q. Indeed, once we have obtained the response function for the exponential case, we can get any polynomial dependence just by differentiating the result with respect to α_i.

We calculate the response function using the basis of coherent states. The coherent state $|z\rangle$ is defined as [14,15]

$$|z\rangle = \mathrm{e}^{za^\dagger}|\Omega\rangle,$$

where $|\Omega\rangle$ denotes the ground state. The coherent states possess the following properties.

(1) Scalar product:

$$\langle z|z'\rangle = \mathrm{e}^{z^* z'}. \tag{7}$$

(2) Unity decomposition:

$$\int |z\rangle\langle z| \frac{\mathrm{d}z}{\langle z|z\rangle} = \mathbb{I}. \tag{8}$$

This property is very important. Coherent states are an overcomplete set of functions and do not form a orthogonal basis, as can be seen from (7). Nevertheless, (8) allows us to expand functions in this basis.

(3) Coherent states are eigenstates of the operator $e^{\alpha a}$, and the operator $e^{\alpha a^\dagger}$ acts on them as a translation operator:

$$e^{\alpha a}|z\rangle = e^{\alpha z}|z\rangle, \qquad e^{\alpha a^\dagger}|z\rangle = |z+\alpha\rangle.$$

Using these properties, we can easily calculate how the operators $e^{\alpha q}$ and $e^{(i/\hbar)H_0 t}$ act on a coherent state,

$$e^{\alpha q}|z\rangle = \exp\left(\alpha\sqrt{\frac{\hbar}{2m\omega_0}}(a^\dagger + a)\right)|z\rangle = \exp\left(\frac{\alpha^2}{2}\frac{\hbar}{2m\omega_0} + \alpha\sqrt{\frac{\hbar}{2m\omega_0}}\right)\left|z + \alpha\sqrt{\frac{\hbar}{2m\omega_0}}\right\rangle,$$

$$e^{-(i/\hbar)H_0 t}|z\rangle = e^{-(i/2)\omega_0 t}|e^{-i\omega_0 t}z\rangle.$$

Here H_0 is given by (6).

We use the initial density matrix

$$\rho_g = \frac{e^{-\beta H_0}}{\mathrm{Tr}\,(e^{-\beta H_0})},$$

and can rewrite (5) in the form

$$S^{(1)}(t_1) = \frac{V_0^2 i/\hbar}{\mathrm{Tr}\,(e^{-\beta H_0})}\int \frac{d^2z}{\langle z|z\rangle}\langle z|e^{\alpha_2 q}(e^{-(i/\hbar)\mathcal{L}t_1}e^{\alpha_1 q^\times})e^{-\beta H_0}|z\rangle,$$

$$S^{(2)}(t_2,t_1) = \frac{V_0^3(i/\hbar)^2}{\mathrm{Tr}\,(e^{-\beta H_0})}\int \frac{d^2z}{\langle z|z\rangle}\langle z|e^{\alpha_3 q}(e^{-(i/\hbar)\mathcal{L}t_2}e^{\alpha_2 q^\times})(e^{-(i/\hbar)\mathcal{L}t_1}e^{\alpha_1 q^\times})e^{-\beta H_0}|z\rangle,$$

$$S^{(3)}(t_3,t_2,t_1) = \frac{V_0^4(i/\hbar)^3}{\mathrm{Tr}\,(e^{-\beta H_0})}$$
$$\times\int \frac{d^2z}{\langle z|z\rangle}\langle z|e^{\alpha_4 q}(e^{-(i/\hbar)\mathcal{L}t_3}e^{\alpha_3 q^\times})(e^{-(i/\hbar)\mathcal{L}t_2}e^{\alpha_2 q^\times})(e^{-(i/\hbar)\mathcal{L}t_1}e^{\alpha_1 q^\times})e^{-\beta H_0}|z\rangle, \tag{9}$$

where $q^\times$ denotes the Liouville-space operator q and $d^2z \equiv d\,\mathrm{Re}\,z\,d\,\mathrm{Im}\,z$. Here α_j relates to the interaction with the jth pulse. We thus obtain a generating function for the nonlinear response.

These expressions can be calculated using the properties of the coherent states, introduced above. The main advantage of the coherent states representation comes from the fact that both $e^{\alpha q}$ and $e^{-(i/\hbar)\mathcal{L}t}$ acting on a coherent state $|z\rangle$ give another coherent state (and not a superposition of states, as would be in the case if we were to use eigenstate representation). As a result, the number of terms in the expression for the response function is considerably reduced.

To present the formulas in a compact form we define the sign operators ε_j that take values + or −. This notation was first introduced in Ref. [18] for a two-level system. It can be shown that each Liouville-space path is characterized by a specific set of ε_j. We thus get

$$S^{(1)}(t_1) = -V_0^2\frac{i}{\hbar}\sum_{\varepsilon_1=\pm}\varepsilon_1\exp[\tfrac{1}{2}(\alpha_1^2+\alpha_2^2)C_+(0) + \alpha_1\alpha_2 C_{\varepsilon_1}(t_1)], \tag{10}$$

$$S^{(2)}(t_2,t_1) = V_0^3\left(\frac{i}{\hbar}\right)^2\sum_{\varepsilon_1,\varepsilon_2=\pm}\varepsilon_1\varepsilon_2$$
$$\times\exp[\tfrac{1}{2}(\alpha_1^2+\alpha_2^2+\alpha_3^2)C_+(0) + \alpha_1\alpha_2 C_{\varepsilon_1}(t_1) + \alpha_2\alpha_3 C_{\varepsilon_2}(t_2) + \alpha_1\alpha_3 C_{\varepsilon_1}(t_2+t_1)], \tag{11}$$

$$S^{(3)}(t_3,t_2,t_1) = -V_0^4\left(\frac{\mathrm{i}}{\hbar}\right)^3 \sum_{\varepsilon_1,\varepsilon_2,\varepsilon_3=\pm} \varepsilon_1\varepsilon_2\varepsilon_3 \exp[\tfrac{1}{2}(\alpha_1^2+\alpha_2^2+\alpha_3^2+\alpha_4^2)C_+(0) + \alpha_1\alpha_2 C_{\varepsilon_1}(t_1)$$
$$+ \alpha_2\alpha_3 C_{\varepsilon_2}(t_2) + \alpha_3\alpha_4 C_{\varepsilon_3}(t_3) + \alpha_1\alpha_3 C_{\varepsilon_1}(t_2+t_1) + \alpha_2\alpha_4 C_{\varepsilon_1}(t_3+t_2) + \alpha_1\alpha_4 C_{\varepsilon_1}(t_3+t_2+t_1)]. \quad (12)$$

Here $C_\pm(t)$ are the two-time autocorrelation functions of the nuclear coordinate ($C_+(t) \equiv \langle q(t)q\rangle$, $C_-(t) \equiv \langle qq(t)\rangle$), defined by

$$C_\pm(t) \equiv \frac{\hbar}{2m\omega_0}\{\cos(\omega_0 t)\coth[\tfrac{1}{2}(\beta\hbar\omega_0)] \pm \mathrm{i}\sin(\omega_0 t)\}. \quad (13)$$

These expressions may be used to calculate the response functions for an arbitrary polynomial dependence of the dipole operator on nuclear coordinates by differentiating them with respect to α_j. If this dependence is linear, all the nonlinear response functions vanish identically[1]. Therefore, the leading term corresponds to a quadratic (q^2) dependence. The Taylor series expansion of the dipole operator may be justified for short-time dynamics of molecular liquids, where the instanteneous normal mode analysis has been shown to reproduce the spectral density observed in femtosecond optical Kerr measurements [16]. For the quadratic interaction we have

$$V(q) = V_0 q^2,$$

we need only to differentiate (10)–(12) twice with respect to every coefficient α_j and then set $\alpha_j = 0$. We then obtain

$$S^{(1)}(t_1) = \frac{V_0^2\hbar}{m^2\omega_0^2}\coth[\tfrac{1}{2}(\beta\hbar\omega_0)]\sin(2\omega_0 t_1), \quad (14)$$

$$S^{(2)}(t_2,t_1) = \frac{2V_0^3\hbar}{m^3\omega_0^3}\coth[\tfrac{1}{2}(\beta\hbar\omega_0)]\{-\cos(2\omega_0 t_1) + \cos[2\omega_0(t_2+t_1)]\}, \quad (15)$$

$$S^{(3)}(t_3,t_2,t_1) = \frac{2V_0^4\hbar}{m^4\omega_0^4}\coth[\tfrac{1}{2}(\beta\hbar\omega_0)]$$
$$\times\{-\sin[2\omega_0(t_3-t_1)] - \sin[2\omega_0(t_3+t_1)] - 2\sin[2\omega_0(t_2+t_1)] + 2\sin[2\omega_0(t_3+t_2+t_1)]\}. \quad (16)$$

In the classical limit these response functions were calculated in Ref. [17][2]. We clearly see from (16) that an echo signal appears for $t_1 = t_3$. Another interesting feature that can be seen from these expressions is that all the quantum effects are contained in the prefactor $\hbar\coth[\frac{1}{2}(\beta\hbar\omega_0)]$, which tends to $2kT/\omega_0$ in the classical $\hbar \to 0$ limit. Note that this is not the case for higher-order response, for example, for the interaction of the q^4 type, in which the $\hbar$-dependence is more complicated.

We now proceed to the detailed study of the behavior of $S^{(2)}$ and $S^{(3)}$, and consider the nonlinear response to lowest order in α. This response is obtained when we expand (11) and (12) in powers of α_j (setting $\alpha_j \equiv \alpha$) and consider the coefficient of the lowest-order term. For $S^{(2)}$ and $S^{(3)}$ this term is proportional to α^4 and α^6, respectively. The explanation of this is very simple: in the case of $S^{(2)}$ there are three interactions with the field, and in the lowest-order nonlinear response we should take one q^2 and two q interactions. Similarly, in the case of $S^{(3)}$ we have either two interactions of the q^2 type and two of q type or one interaction of the q^3 type and three of the q type. In that case the response contains more terms than for pure q^2 case, and is written as

$$S^{(2)}(t_2,t_1) = \frac{4V_0^3\alpha^4}{\hbar^2}C''(t_2)[C''(t_1) + C''(t_1+t_2)], \quad (17)$$

[1] This can be easily seen from the Drude oscillator equation of motion, which is linear.

[2] Eqs. (33) and (34) in Ref. [17] are incorrect. They should be replaced by Eqs. (15) and (16) of this Letter.

$$S^{(3)}(t_3,t_2,t_1)=\frac{8V_0^4\alpha^6}{\hbar^3}C''(t_3)[C''(t_2)+C''(t_2+t_3)][C''(t_1)+C''(t_1+t_2)+C''(t_1+t_2+t_3)], \quad (18)$$

where $C''(t)$ is the imaginary part of $C_+(t)$. Using the explicit form of $C''(t)$, we can write

$$S^{(2)}(t_2,t_1)=\frac{V_0^3\alpha^4}{m^2\omega_0^2}\{\cos(\omega_0 t_1)-\cos[\omega_0(t_1+t_2)]+\cos[\omega_0(t_1+2t_2)]-\cos[\omega_0(t_1-t_2)]\}, \quad (19)$$

$$\begin{aligned}S^{(3)}(t_3,t_2,t_1)=\frac{V_0^4\alpha^6}{m^3\omega_0^3}\{&\sin[\omega_0(t_1-t_2)]+\sin[\omega_0(t_1+t_2)]-2\sin[\omega_0(t_1-t_3)]+2\sin[\omega_0(t_1+t_3)]\\&-\sin[\omega_0(t_1-2t_3)]+2\sin[\omega_0(t_1+2t_2)]-\sin[\omega_0(t_1-t_2-t_3)]\\&+\sin[\omega_0(t_1+t_2-t_3)]+\sin[\omega_0(t_1-t_2+t_3)]-\sin[\omega_0(t_1+t_2+t_3)]\\&-\sin[\omega_0(t_1-t_2-2t_3)]-\sin[\omega_0(t_1+t_2+2t_3)]+\sin[\omega_0(t_1+2t_2-t_3)]\\&-\sin[\omega_0(t_1+2t_2+2t_3)]+2\sin[\omega_0(t_1+2t_2+3t_3)]+\sin[\omega_0(t_1+2t_2)]\}. \quad (20)\end{aligned}$$

These results correspond to a single oscillator. In order to mimic the spectral density of molecular liquids, we need to use a continuous distribution of oscillators. It is possible to represent this spectral density in terms of a multimode Brownian oscillator model (Eq. (23), see below). The system can therefore be viewed either as infinite number of undamped oscillators, or as a superposition of few damped Brownian oscillators. The two pictures are mathematicaly identical. The application to a continuous distribution of oscillators will be made in the Section 4.

4. Response of inhomogeneous distribution of oscillators

Consider now the case when the coupling is a function of a particular combination of nuclear modes,

$$q=\sum_n \rho_n q_n.$$

In the continuous limit, we replace ρ_n by a distribution function $\rho(\omega_0)$ and then formulas (10)–(12) should be rewritten with a substitution

$$C_\pm(t)\longrightarrow\int_0^\infty d\omega_0\ \rho(\omega_0)\eta^2(\omega_0)C_\pm(t,\omega_0), \quad (21)$$

where $\eta(\omega_0)$ is the coupling coefficient (each constant factor α_j is replaced by $\alpha_j\eta(\omega_0)$).

This is a coherent 'homogeneous' mechanism. If we simply assume an inhomogeneous distribution of oscillators, we have

$$S^{(n)}=\int_0^\infty d\omega_0\ f(\omega_0)S^{(n)}(t_n,\ldots,t_1;\omega_0). \quad (22)$$

It was shown in Ref. [5] that in the linear response it is impossible to distinguish between the two mechanisms, and higher-order response needs to be studied.

In this section we consider inhomogeneous broadening. We assume that the oscillator mode ω_0 is distributed around some central frequency ω_1 with the half-width γ_1. The specific form of this distribution that will be used below is taken to be of the Brownian oscillator form

$$f(\omega_0,\omega_1,\gamma_1)=\frac{1}{2\pi}\frac{\omega_0\gamma_1}{(\omega_1^2-\omega_0^2)^2+\omega_0^2\gamma_1^2}. \quad (23)$$

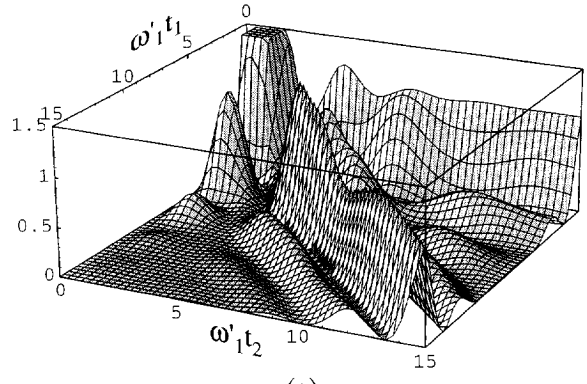

Fig. 1. (a) Response function $S^{(2)}(t_2, t_1)$. The squared absolute value of $S^{(2)}$ is shown. (b) Double-sided Feynman diagrams representing the terms that produce the echo signal at $t_1 = t_2$ for $S^{(2)}$.

The response is then calculated by averaging (19) and (20) with the distribution function (23) as shown in (22). Necessary integrals can be now calculated in the underdamped limit $\omega_1 \gg \frac{1}{2}\gamma_1$.

We obtain for second-order response

$$S^{(2)}(t_2, t_1) = \frac{V_0^3 \alpha^4}{4m^2(\omega_1')^2}\{\cos(\omega_1' t_1)e^{-\gamma_1 t_1} - \cos[\omega_1'(t_1 + t_2)]e^{-\gamma_1(t_1+t_2)} + \cos[\omega_1'(t_1 + 2t_2)]e^{-\gamma_1(t_1+2t_2)} - \cos[\omega_1'(t_1 - t_2)]e^{-\gamma_1|t_1-t_2|}\}. \tag{24}$$

where $\omega_1' = \sqrt{\omega_1^2 - (\frac{1}{2}\gamma_1)^2}$. The third-order response can be written similar to (20), but each sine will be replaced by a cosine multiplied by a decaying exponential factor with the same time argument.

In Fig. 1a we show the absolute squared value of the response function, $|S^{(2)}|^2$, as a function of t_1 and t_2. The parameter γ_1 is taken as $\gamma_1 = \frac{1}{2}\omega_1$. It is clearly seen that for $t_1 = t_2$ the response does not vanish for large times, resulting in the photon echo signal. A nontrivial point here is that the echo signal is present in the second-order response function, while in the usual two-level model of nuclear system it appears only in the third order. The corresponding double-sided Feynman diagrams are shown in Fig. 1b. Note, that as a result of each interaction of the q type the system moves either one level up or one level down, whereas the q^2 interaction either moves the system by two levels or does not change its state at all.

Note that if all the interactions were of the q^2 type, the echo signal in $S^{(2)}$ would not exist, appearing only in $S^{(3)}$; this is clearly seen from (15) and (16).

The third-order response function $S^{(3)}$ shows a similar behavior. In the general case, eight photon echo signals can be identified,

$$t_1 = t_2, \quad t_1 = t_3, \quad t_1 = 2t_3, \quad t_1 = t_2 + t_3, \quad t_1 = t_3 - t_2, \quad t_1 = t_2 - t_3,$$
$$t_1 = t_2 + 2t_3, \quad t_1 = t_3 - 2t_2. \tag{25}$$

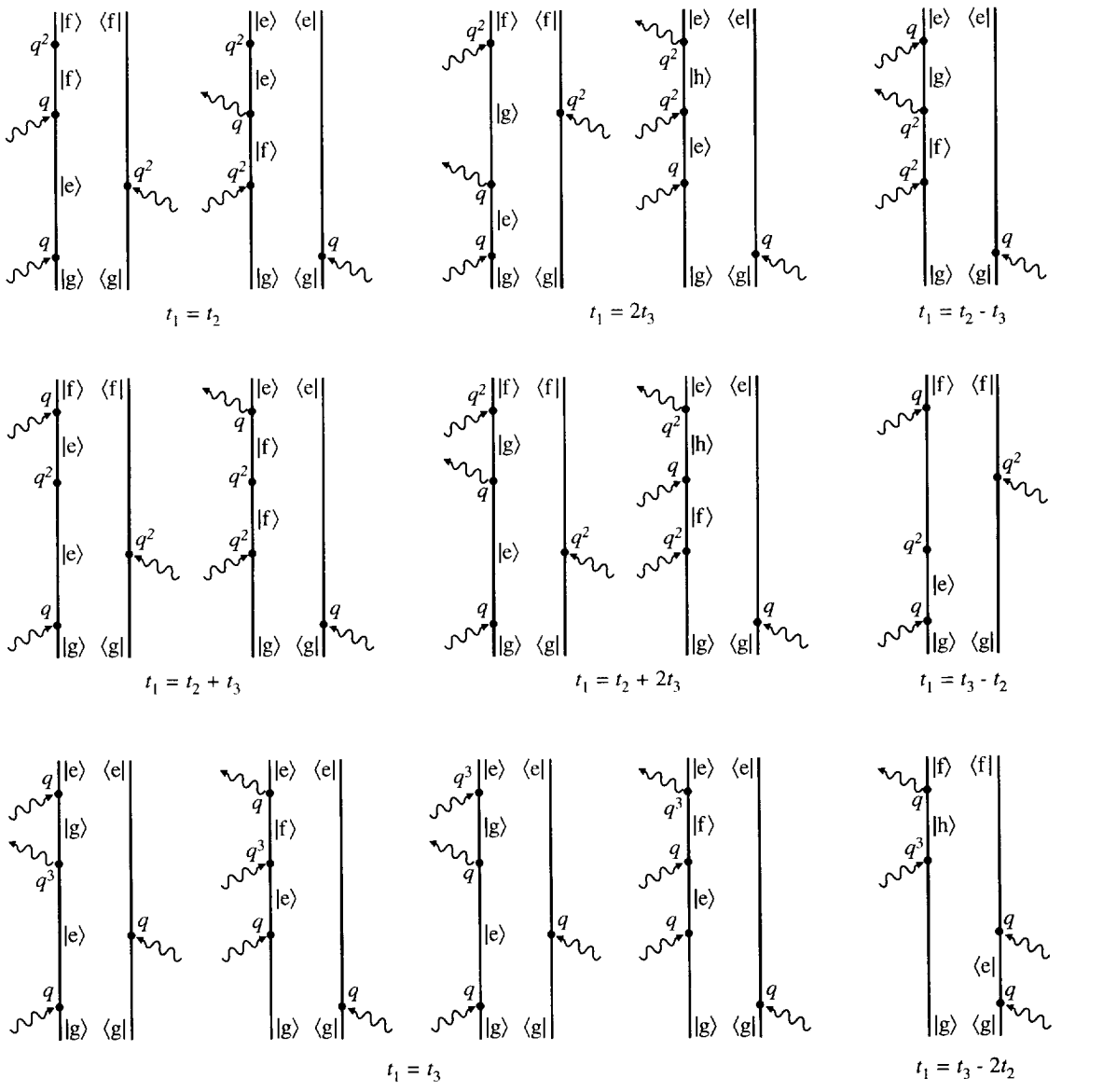

Fig. 2. Double-sided Feynman diagrams representing the terms that produce the echo signals in $S^{(3)}$ when t_1, t_2, and t_3 satisfy conditions (25).

The Feynman diagrams corresponding to these echo signals are presented in Fig. 2. Only half of the diagrams is shown in this figure; for each diagram there exists a counterpart obtained by interchanging the bra and ket interactions with the field (except for the last interaction). Note also that as a result of the q^3 type interaction, the system can move by either one level (terms $aa^\dagger$ or $a^\dagger a$) or by three levels (terms a^3 and $(a^\dagger)^3$). As before, $|g\rangle$ denotes the ground state, and $|e\rangle$, $|f\rangle$, and $|h\rangle$ stand for the first, second, and third excited levels, respectively.

Using these diagrams, it is easy to see which coherences are responsible for each echo signal. For example, if we examine the first diagram in Fig. 2, we see that during the period t_1 the system is in the coherence eg, gaining the phase factor $\exp(i\omega_{eg}t_1)$, and during the period t_2 in ef, receiving the phase $\exp(-i\omega_{fe}t_2)$. Since

Table 1
Coherencies corresponding to different echo signals

Echo signal	Coherence
$t_1 = t_2$	$\langle \mathcal{G}_{ef}(t_2)\mathcal{G}_{eg}(t_1)\rangle$
$t_1 = 2t_3$	$\langle \mathcal{G}_{gf}(t_3)\mathcal{G}_{eg}(t_1)\rangle$
$t_1 = t_2 + t_3$	$\langle \mathcal{G}_{ef}(t_3)\mathcal{G}_{ef}(t_2)\mathcal{G}_{eg}(t_1)\rangle$
$t_1 = t_2 + 2t_3$	$\langle \mathcal{G}_{gf}(t_3)\mathcal{G}_{ef}(t_2)\mathcal{G}_{eg}(t_1)\rangle$
$t_1 = t_2 - t_3$	$\langle \mathcal{G}_{ge}(t_3)\mathcal{G}_{fe}(t_2)\mathcal{G}_{ge}(t_1)\rangle$
$t_1 = t_3 - t_2$	$\langle \mathcal{G}_{ef}(t_3)\mathcal{G}_{eg}(t_2)\mathcal{G}_{eg}(t_1)\rangle$
$t_1 = t_3 - 2t_2$	$\langle \mathcal{G}_{hf}(t_3)\mathcal{G}_{gf}(t_2)\mathcal{G}_{ge}(t_1)\rangle$
$t_1 = t_3$	$\langle \mathcal{G}_{ge}(t_3)\mathcal{G}_{eg}(t_1)\rangle$, $\langle \mathcal{G}_{fe}(t_3)\mathcal{G}_{ge}(t_1)\rangle$

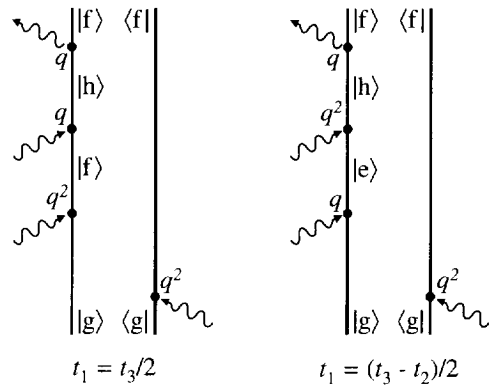

Fig. 3. Examples of Feynman diagrams that could contribute to echo signals in $S^{(3)}$ at $t_1 = \frac{1}{2}t_3$ and $t_1 = \frac{1}{2}(t_3 - t_2)$ as indicated. Due to the interference with other diagrams (not shown), these contributions cancel, and no such echoes are observed in Figs. 4 and 5.

for the harmonic oscillator $\omega_{eg} = \omega_{fe}$, we get a nonvanishing response after the averaging over the distribution of ω_0 if $t_1 = t_2$. Thus we can write the Green functions corresponding to each echo signal (and Feynman diagram). These results are summarized in Table 1.

Not all the possible paths are shown in Fig. 2. For example, we can consider the diagrams given in Fig. 3. They should give an echo signal when $t_1 = \frac{1}{2}t_3$ or $t_1 = \frac{1}{2}(t_3 - t_2)$. Nevertheless, when we collect all the terms that produce each of these echo signals, they are cancelled, and give no contribution to the response. This illustrates that not every sequence of interactions gives a contribution to the response. It may be shown directly that when we have two q^2 and two q interactions, only three permutations (out of six) remain: (q, q^2, q^2, q), (q, q^2, q, q^2), and (q, q, q^2, q^2). Similarly, when we have one q^3 and three q interactions, the remaining paths are (q, q, q^3, q) and (q, q, q, q^3).

In Fig. 4 we present the response $S^{(3)}(t_3, t_2, t_1)$ for the case $t_2 = t_3$. Three echo signals can be clearly seen: $t_1 = t_3$, $t_1 = 2t_3$, and $t_1 = 3t_3$. Both a three-dimensional and contour plots are presented. For the calculations we used $\gamma_1 = \frac{1}{2}\omega_1$. In Fig. 5 we display the response $S^{(3)}(t_3, t_2, t_1)$ for the case when t_2 is constant: $\omega_1' t_2 = 3\pi$. In this case all the eight echo signals listed in (25) can be easily distinguished.

The calculations presented in Figs. 1, 4, and 5 used a specific model of a harmonic system, and the dipole had the form $V(q) = \alpha q + \frac{1}{2}\alpha^2 q^2$. We believe, however, that the qualitative effects predicted in this Letter, namely, the appearence of new types of echoes at specific combinations of time intervals, are not limited to the particular model used. One major difficulty in this type of experiments is to satisfy the phase-matching condition. This is crucial in order to distinguish between various nonlinear signals that appear in closely lying directions.

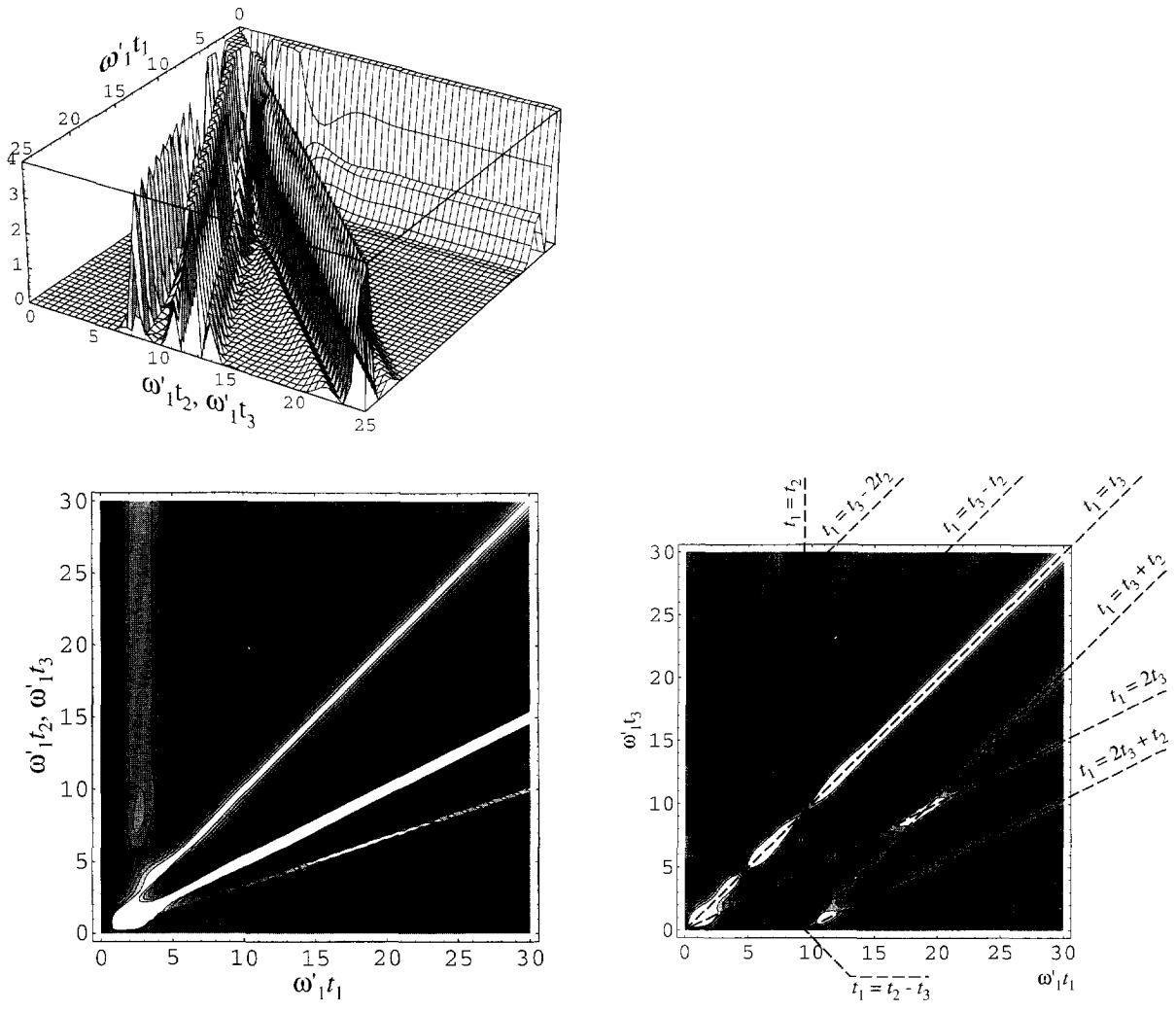

Fig. 4. (a) The signal $|S^{(3)}(t_3, t_2, t_1)|^2$ for $t_2 = t_3$. (b) The response function $S^{(3)}(t_3, t_2, t_1)$ for $t_2 = t_3$. The grey background indicates the magnitude of $S^{(3)}$ (dark (light) regions correspond to positive (negative) values).

Fig. 5. Response function $S^{(3)}(t_3, t_2, t_1)$ for the case $\omega'_1 t_2 = 3\pi$. All the eight echo signals listed in (25) are clearly seen.

We further note that photon echo is an ideal time domain technique which requires no spectral resolution. In the impulsive mode considered in this Letter, the signal is proportional to $|S^{(3)}|^2$. The connection between the response functions and the measurements is then most transparent. However, the comparison with experiments conducted using finite pulses may require convoluting the response functions with the pulse envelopes. This may limit the types of nuclear motions that can be resolved [19]. Current optical Kerr measurements can easily cover the spectral range of 0 to 1000 cm^{-1}.

In conclusion we point out the connection between the techniques discussed in the article, which use infrared pulses and probes vibrational transitions directly, and the optical off-resonant experiments. In the latter case we may rewrite the problem using the effective Hamiltonian what results in replacing the term $E(\boldsymbol{r}, t)V$ in the Hamiltonian (1) by $E^2(\boldsymbol{r}, t)\alpha(q)$, where $\alpha(q)$ is the electronic polarizability. This analysis was performed in

Ref. [5] using the path-integral techniques. Assuming the same dependencies of the electronic polarizability on nuclear coordinate q, we can obtain same formulas for the response; the only difference is that the order of nonlinearities becomes higher: the nth order in the infrared technique turns into the $(2n+1)$th order in optical measurements. On the other hand, the technology for optical experiments is more advanced than for the infrared. Each technique has its own advantages and both of them could successfully complement each other.

Acknowledgement

We wish to thank Dr. V. Chernyak for many helpful discussions. The support of the National Science Foundation and the Air Force Office of Scientific Research is gratefully acknowledged.

References

[1] W.E. Moerner, ed., Persistent spectral hole burning. Science and applications (Springer, Berlin, 1988).
[2] A.M. Stoneham, Rev. Mod. Phys. 41 (1969) 82.
[3] S. Mukamel, Principles of nonlinear optical spectroscopy (Oxford Univ. Press, Oxford, 1995).
[4] M. Orrit, J. Bernard and R.I. Personov, J. Phys. Chem. 97 (1993) 10256.
[5] Y. Tanimura and S. Mukamel, J. Chem. Phys. 99 (1993) 9496.
[6] R.I. Personov, E.I. Al'shits and L.A. Bykovskaya, Opt. Commun. 6 (1972) 169.
[7] D. Haarer and R.J. Silbey, Phys. Today 43 (1990) 58.
[8] A.A. Villaeys, J.C. Vallet, H. Ma and S.H. Lin, Phys. Rev. A 16 (1992) 5959.
[9] N.A. Kurnit, I.D. Albella and S.R. Hartmann, Phys. Rev. Letters 13 (1964) 567;
I.D. Albella, N.A. Kurnit and S.R. Hartmann, Phys. Rev. 141 (1966) 391.
[10] E.T.J. Nibbering, D.A. Wiersma and K. Duppen, Phys. Rev. Letters 66 (1991) 2464.
[11] M. Cho, G.R. Fleming and S. Mukamel, J. Chem. Phys. 98 (1993) 5314.
[12] M. Cho, M. Du, N.F. Scherer, G.R. Fleming and S. Mukamel, J. Chem. Phys. 99 (1993) 2410.
[13] Y.R. Shen, The principles of nonlinear optics (Wiley, New York, 1984).
[14] R.J. Glauber, Phys. Rev. 131 (1963) 2766.
[15] J.R. Klauder and B.-S. Skagerstam, Coherent states – applications in physics and mathematical physics (World Scientific, Singapore, 1985).
[16] J.E. Adams and R.M. Stratt, J. Chem. Phys. 93 (1990) 1332;
M. Cho, G.R. Fleming, S. Saito, I. Ohmine and R.M. Stratt, J. Chem. Phys. 100 (1994) 6672.
[17] J.A. Leegwater and S. Mukamel, J. Chem. Phys. 102 (1995).
[18] S. Chakravarty and A.J. Leggett, Phys. Rev. Letters 52 (1984) 5.
[19] D. McMorrow and W.T. Lotshaw, Chem. Phys. Letters 174 (1990) 85.